M. H. Sanad*, Ayman B. Farag*, F. A. Marzook and Sudip Kumar Mandal

Preparation, characterization, and bioevaluation of ^{99m}Tc-famotidine as a selective radiotracer for peptic ulcer disorder detection in mice

https://doi.org/10.1515/ract-2021-1105
Received September 16, 2021; accepted October 13, 2021; published online November 2, 2021

Abstract: This work focuses on tracking peptic ulcer localized in mice. The formation of a [^{99m}Tc]dithiocarbamate of famotidine complex at optimum conditions of reaction temperature (37 °C), reaction time (30 min), pH of the reaction mixture (5), amount of substrate (100 μg), amount of reducing agent (tin (II) content, 50 μg), was achieved using radioactive Tc-^{99m} (250–400 MBq), with labelling yield of 98% and high radiochemical purity. The *in-vitro* stability of [^{99m}Tc]dithiocarbamate of famotidine complex was shown to be high in rat serum for up to 8 h. Normal and ulcerated mice were used in biodistribution studies. Famotidine works by blocking histamine-2-receptor antagonists (H_2RAs). The high absorption of [^{99m}Tc]dithiocarbamate of famotidine complex in stomach in amount of 27.15% injected dose/g organ (ID/g) observed in ulcerated mice for up to 24 h demonstrated its usefulness as a novel radiotracer for stomach imaging.

Keywords: complex; biodistribution; famotidine; histamine-2-receptor; stomach ulcers imaging.

1 Introduction

Famotidine, also known as 3-[[2-(diaminomethylideneamino)-1,3-thiazol-4-yl]methylsulfanyl]-*N*′-sulfamoylpropanimidamide, is one of the drugs that can be used to reduce gastric acid secretion [1–3]. Many radiotracers have been used to image stomach ulcers [4–12]. However, there is a critical point to consider regarding the radiotracer's follow-up. Because famotidine has a high affinity for specific stomach receptors such as histamine-2-receptor antagonists (H2RAs), it can be employed as a possible marker in stomach ulcer imaging. A stomach ulcer is known to cause mucous erosions of 0.5 cm or more in an area of the gastrointestinal tract that is usually acidic and thus extremely painful. *Helicobacter pylori* (*H. pylori*) is widely recognized as the most common cause of peptic ulcers [13–15]. [^{99m}Tc]nitrido complexes are regarded as one of the important radiotracers achieved, playing an essential role in radiocomplexation and diagnostic procedures in nuclear medicine. In several features, including chemical and biological properties, the [^{99m}Tc]nitrido core outperforms the [^{99m}Tc]oxo core. Because the nitrido (N^{-3}) ligand is a powerful π-electron donor, it can stabilize its [^{99m}Tc]nitrido core, making these labelled compounds pyrogen free [16]. The goal of this study is to prepare a dithiocarbamate of famotidine (Figure 1) that reacts with [^{99m}Tc]nitrido core to give [^{99m}Tc]dithiocarbamate of famotidine complex of the postulated structure given in Figure 2 capable of overcoming the aforementioned critical threshold. In a biodistribution investigation, two Swiss Albino mouse models (normal and stomach ulcer models) were used to evaluate the quantity of this labelled compound, [^{99m}Tc]nitrido-famotidine complex, in its target organ (stomach ulcer) for a long period of time of up to 24 h.

2 Experimental

2.1 Materials and methods

Famotidine, succinicdihydrazide, propylenediaminetetraacetic acid (PDTA), aqueous ammonia solution, and carbon disulfide were purchased from Sigma-Aldrich, St. Louis, MO, USA. Unless otherwise specified, all chemicals were of analytical or clinical grade and were used directly without further purification. Elemental analyses were performed at the National Research Centre's Micro Analytical Center (Cairo, Egypt) using an ELEMENTAR viro EL instrument from Germany. Mass spectra were recorded on a Shimadzu GCMS-QP1000 EX mass spectrometer at 70 eV. The ^{1}H and ^{13}C NMR spectra were recorded on a Varian Mercury VXR-350 MHz spectrometer after being dissolved in deuterated chloroform ($CDCl_3$) or dimethylsulphoxide (DMSO-d_6), and the chemical shifts were measured as δ (ppm) down field from

***Corresponding authors: M. H. Sanad**, Labeled Compounds Department, Hot Laboratories Center, Egyptian Atomic Energy Authority, P.O. Box 13759, Cairo, Egypt; and Department of Physics and Engineering Mathematics, Faculty of Engineering, Ain Shams University, P.O. Box 11566, Cairo, Egypt,
E-mail: drsanad74@gmail.com; and **Ayman B. Farag**, Pharmaceutical Chemistry Department, Faculty of Pharmacy, Ahram Canadian University, Giza, Egypt, E-mail: abfarag81@yahoo.com
F. A. Marzook, Labeled Compounds Department, Hot Laboratories Center, Egyptian Atomic Energy Authority, P.O. Box 13759, Cairo, Egypt, E-mail: fawzymarzouk@yahoo.com
Sudip Kumar Mandal, Department of Pharmaceutical Chemistry, Dr. B. C. Roy College of Pharmacy and Allied Health Sciences, Durgapur 713 206, West Bengal, India,
E-mail: gotosudip79@gmail.com

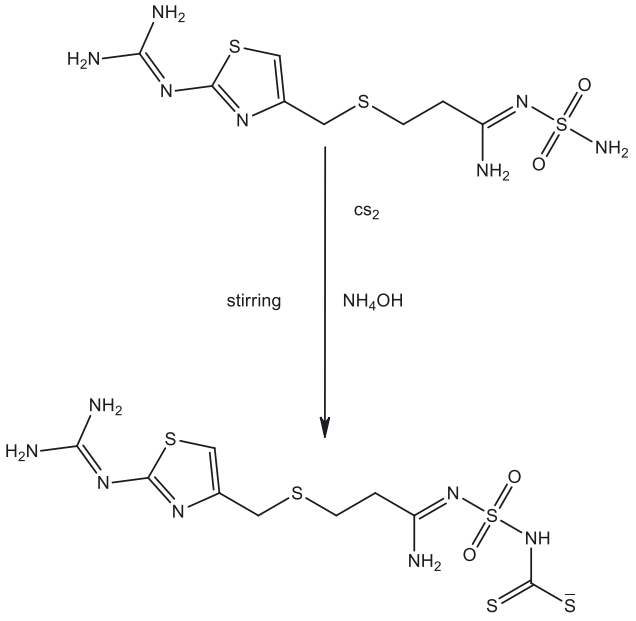

Figure 1: Schematic representation of synthesis of dithiocarbamate of famotidine.

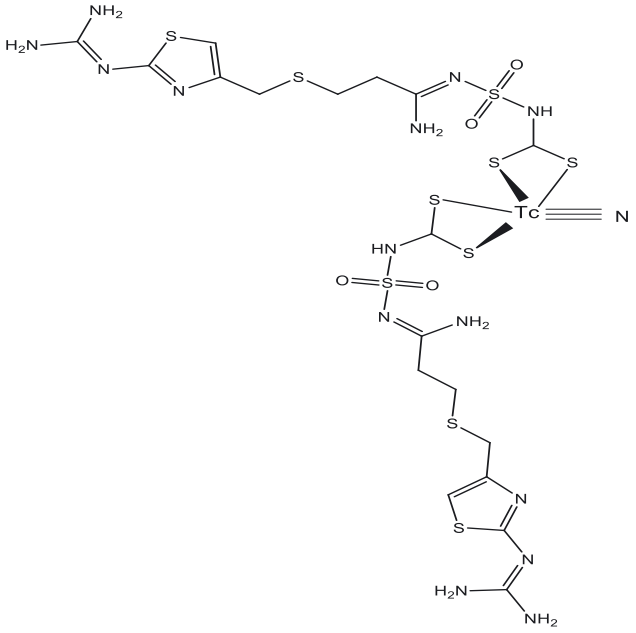

Figure 2: Structure of [99mTc]dithiocarbamate of famotidine complex.

tetramethylsilane (TMS) as an internal standard. A well-type NaI scintillation γ-Counter Model Scalar Ratemeter SR7 (Nuclear Enterprises Ltd., USA) was used for radioactivity measurement. [^{99m}Tc] ($T_{1/2}$ = 6 h, $E\gamma$ = 140 keV) was eluted from a ^{99M}o-^{99m}Tc generator (RPF, Egyptian Atomic Energy Authority, Inshas, Egypt). The radiotracer, [^{99m}Tc]dithiocarbamate of famotidine complex, was purified by high performance liquid chromatography (Shimadzu HPLC) equipped with a UV detector SpD-6A, a reversed phase Waters symmetry C_{18} (10 µm, 250 × 4.6 mm) column (Waters Corporation, Milford, MA, USA), a Lischrosorb column (5 µm, 150 × 4.6 mm) (Merck), a LC-9A pump, DGU-2A degasser, LKB Bromma fraction collector, and C-R4A chromatopac data processor. RP-HPLC analysis was performed using isocratic elution of water:acetonitrile:triethylamine (80:10:10, v/v/v; pH 6.0) at a column temperature maintained at 25 °C. The flow rate was set at 1.0 mL/min with the detection wavelength of 278 nm [17]. The radiotracer, [^{99m}Tc]dithiocarbamate of famotidine complex, was collected with a fraction collector and its activity was measured with a well type NaI (Tl) crystal connected to a single channel analyser. In addition, the [^{99m}Tc]nitrido core was determined using a reaction through the HPLC column of RP-18 (Lichrosorb, 5 µm, 150 × 4.6 mm) using the gradient elution of water (solvent A) and acetonitrile (solvent B) injected through this column. Starting with 100% A/0% B with a linear gradient to 0% A/100% B from 0 to 30 min. The flow rate was adjusted to 1.0 mL/min [17–19]. Thin layer chromatography (TLC) aluminum sheets (20 × 25 cm) SG-60 F_{254} were supplied by Merck. The core of [^{99m}Tc]nitrido was detected using TLC sheets, marked 2 cm from the base and lined into fragments 1 cm each up to 14 cm using a combination of two different solvent systems of normal saline 0.9% and methanol: chloroform (1:9 v/v). A spot (5 µL) from the reaction mixture was applied with a micropipette, and then the strip was developed in an ascending manner in a closed jar filled with N_2 gas to prevent oxidation of the labelled spot. The strip was developed using the eluting solvent system, dried, cut into 1 cm segments, and the radioactivity associated with each segment was measured using a well-type NaI(Tl) detector. The colloidal impurities were separated by filtration of the reaction mixture through a 0.22 µm Millipore filter at a suitable pressure [18–20].

2.2 Synthesis of dithiocarbamate of famotidine

It was carried out by adding 0.5 mL of carbon disulfide solution in ethanol (1:4 v/v) to a pre-cooled solution of famotidine (5 mg, 14.82 mol) in aqueous ammonia (2 mL) at 0 °C with stirring. The resulting mixture was stirred overnight at room temperature. After the reaction was completed, the dithiocarbamate famotidine product was subjected to vacuum process to eliminate solvent and to allow re-crystallization. Thereafter it was characterized by ^{1}H NMR, mass spectrometry, and elemental analysis. The yield of dithiocarbamate famotidine was 49%, and the melting point was (188–190 °C).

2.3 Characterization of dithiocarbamate famotidine

Mass spectrometry, ^{1}H NMR and elemental analysis confirmed the synthesis of dithiocarbamate famotidine [$C_9H_{14}N_7O_2S_5$], with a molecular ion peak at m/z 380.62 [M–S]. The obtained results of elemental analysis were C 26.19; H 3.42; and N 23.75%, which were in good agreement with the calculated elemental analysis as C 26.18, H 3.39, and N 23.76%. The ^{1}H NMR (DMSO-d_6) spectrum showed 14 proton resonances in the molecule at δ (ppm) 8.44 (s, 2H, NH_2–C=N–SO_2), 2.45 (t, 2H, S–CH_2–CH_2–C=N), 2.73 (t, 2H, S–CH_2–CH_2–C=N), 3.62 (s, 2H, C–CH_2–S), 8.51 (s, 4H, 2NH_2–CH=N), and 7.25 (s, 1H), aromatic (s, 1H, 2NH–CS_2). The ^{13}C NMR (DMSO-d_6) spectrum showed the presence of nine carbon resonances in the molecule at δ (ppm) 24.5, 31.8, 37.9, 115.11, 152.5, 154.9, 157.33, 168.23, and 201.7.

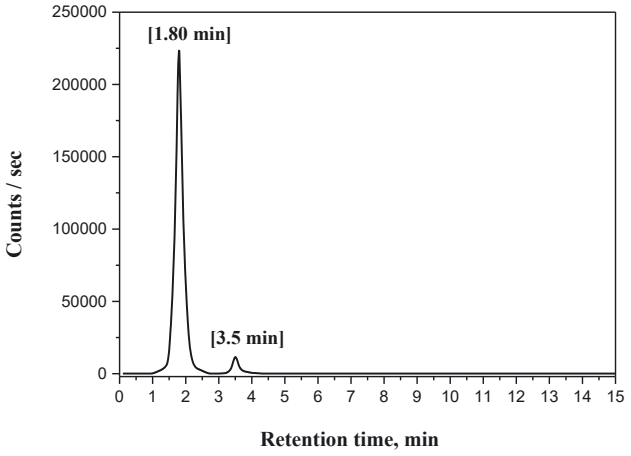

Figure 3: HPLC of ^{99m}Tc-Nitride core >99%, t_R = 1.80 min, (mean yield % ± SD, n = 3).

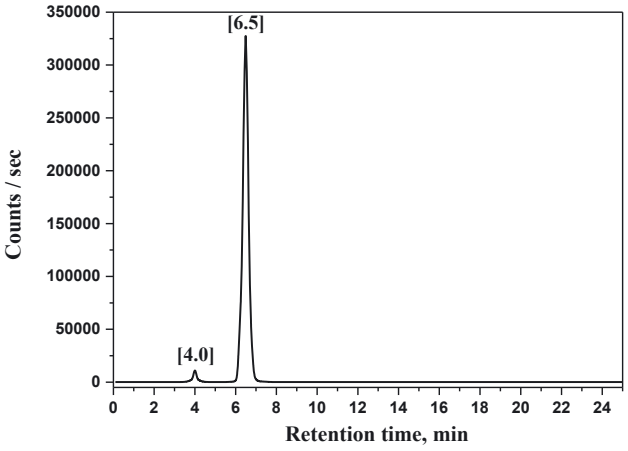

Figure 4: HPLC of [^{99m}Tc]dithiocarbamate of famotidine complex >98%, t_R = 6.50 min (mean yield % ± SD, n = 3).

2.4 Synthesis of technetium-99m nitride core

It was done using 50 µL (50 µg) of $SnCl_2 \cdot 2H_2O$ in aqueous HCl, adding 5 mg of succinicdihydrazide and 5 mg of PDTA, sodium dihydrogen phosphate (0.5 mg), and disodium hydrogen phosphate (5.8 mg). The mixture was then kept at ambient temperature for 30 min after the addition of 1 mL of pertechnetate (37 MBq, 1 mCi) [21–33]. As a result, the reaction mixture yielded a technetium-99m nitride core, which was characterized using TLC and HPLC (Figure 3). The t_R value of 1.8 min is nearly close to the values of 1.86 and 1.85 min reported in Refs. [20] and [18], respectively. Although it does not convincingly establish the structure, it gives us confidence to assume the suggested structure.

2.5 Factors affecting the radiolabelling yield

Several parameters, including ambient temperature, substrate concentration (50–1000 µg), reaction mixture pH (2–12), and reaction time (1–120 min) were considered, as in previous reports [18–20]. To achieve the best results (high radiolabelling yield), each of the investigated parameters of the labelling process was optimized using trial and error method. The experiment was repeated until the optimal conditions were attained, with all factors kept at optimum, and altering only the factor under study, till the optimization process was completed.

2.6 Preparation of the radiotracer: [^{99m}Tc] dithiocarbamate of famotidine complex

It was synthesized by combining a 0.5 mL solution of freshly prepared technetium-99m nitride core (15–20 MBq) with 100 µg of famotidine dissolved in ethanol (0.5 mL, 1 mg:1 mL). The product was vortexed vigorously and then the mixture kept at ambient temperature at pH 5 for 30 min reaction time. The radiochemical purity of the complex, [^{99m}Tc]dithiocarbamate of famotidine was determined using RP-HPLC as shown in Figure 4. The product is ≥98% pure; its suggested structure is based again on HPLC data.

2.7 Serum stability

It was performed by adding 0.2 mL of radiotracer, [^{99m}Tc]dithiocarbamate of famotidine complex, to 1.7 mL freshly prepared rat serum. The procedure was carried out by allowing the radiotracer to stand at room temperature for 24 h. About 50 µL aliquots were taken from the total mixture and analysed by HPLC to detect the % of the tracer remaining in the original form [18–20]. The results are given in Table 1.

2.8 Biodistribution study

All animal experiments were carried out with the approval of the Ethics Committee of the institute. The biodistribution of the radiotracer, [^{99m}Tc] dithiocarbamate of famotidine complex was investigated using six groups (5 mice for each group to give 30 mice in total for whole study, n = 5). Each mouse was of the institute of famotidine complex (after purifying by HPLC) via the tail vein. Animals were sacrificed at various points after injection (30 min, 60 min, 120 min, 240 min, 8 h, and 24 h). All organs were isolated and the biodistribution of [^{99m}Tc]dithiocarbamate of famotidine complex in all organs was examined in comparison to a standard solution of the labelled substrate [34], which eliminated any correction due to decay of the radionuclide. The Student's t-test was used to assess data differences. The results of the 2-tailed test for p are reported and all findings are expressed as mean SEM. The level of significance was set at $p < 0.05$.

Table 1: *In-vitro* stability in rat serum of [^{99m}Tc]dithiocarbamate of famotidine complex.

Time (h)	[^{99m}Tc]dithiocarbamate of famotidine (%)	[^{99m}Tc]nitrido core (%)
3	98.2 ± 0.15	1.8 ± 0.98
6	97.5 ± 0.12	2.5 ± 0.72
9	97.0 ± 0.81	3.0 ± 0.79
12	95.0 ± 0.18	5.0 ± 0.88
24	94.0 ± 0.76	6.0 ± 0.65

Values represent the mean ± SEM, n = 3.

2.9 Blocking study

Various concentrations of unlabelled famotidine ranging from 0 to 1000 µg were used. Unlabelled famotidine was injected into the mice 30 min before the administration of the radiotracer, [^{99m}Tc]dithiocarbamate of famotidine complex, and the percent of ulcerated stomach uptake was assessed 30 min post injection of the [^{99m}Tc]dithiocarbamate of famotidine complex (n = 5) [27–35].

2.10 Ulceration method of the mice stomach

There are numerous methods for inducing stomach ulcers in laboratory animals. The simplest way of inducing stomach ulcers in mice is to administer 1 mL HCl (or) acidified ethanol/mice intravenously (0.1 mL HCl/ethanol per 10 g body weight and 55–65% 150 mmol HCl) [35]. After 1–2 h, the stomach distended and ulcer symptoms appeared [4–14].

3 Results and discussion

3.1 Evaluation of percent radiotracer and the purity of the labelled compound, [^{99m}Tc] dithiocarbamate of famotidine complex

Most of the colloidal impurities such as [^{99m}Tc]-tin-colloid, technetium dihydroxide, stannous dihydroxide, or technetium tetrahydroxide were eliminated using a 0.22 µm Millipore filter. There are four main species, [^{99m}Tc]nitride core, [^{99m}Tc]dithiocarbamate of famotidine complex, $[^{99m}TcO_4]^-$ and the rest colloid ($[^{99m}Tc]O_2{\cdot}nH_2O$); their contributions were estimated using the TLC method described in earlier reports [24, 25]. In the first mobile phase (saline), free pertechnetate, colloid (if any, $[^{99m}Tc]O_2{\cdot}nH_2O$) and the complex ([^{99m}Tc]dithiocarbamate of famotidine complex) remained at the origin, Rf 0–0.1, but the intermediate core ([^{99m}Tc]nitride core) migrated to the front, Rf 0.7–1.0. In the second mobile phase (methanol:chloroform, 1:9 v/v), the complex ([^{99m}Tc]dithiocarbamate of famotidine complex) migrated to the front, Rf 0.9–1.0, but the free pertechnetate, ($[^{99m}TcO_4]^-$), colloid, if any ($[^{99m}Tc]O_2{\cdot}nH_2O$), if any, and intermediate core ([^{99m}Tc]nitride core) remained at the origin, Rf 0–0.1. In addition, the purity of the radiotracer [^{99m}Tc]dithiocarbamate of famotidine complex and its core was also confirmed by HPLC data. The purity of the core intermediate ([^{99m}Tc]nitride core) was more than 99% at R_t value of 1.80 min, whereas the R_t value of free pertechnetate was 3.5 min (Figure 3). On the other hand, the R_t values of [^{99m}Tc]dithiocarbamate famotidine complex and the free pertechnetate were 6.5 and 4.0 min, respectively (Figure 4).

3.2 Reaction optimization

The parameters affecting the labelling process were optimized to achieve the maximum radiolabelling yield at ambient temperature. As shown in Figure 5, the high radiolabelling yield of the complex (98.0%) was observed with substrate concentrations of 100 µg of famotidine and 7.4 MBq of [^{99m}Tc]nitride core, the rest of the factors being constant [26]. Furthermore, the pH of the reaction mixture is regarded as a crucial parameter in the radiolabelling process and pH 5 was found to be optimal for this process (Figure 6), possibly through improvement in the stability of the [^{99m}Tc]dithiocarbamate of famotidine complex [36–40]. The effective reaction time (Figure 7) was also investigated; a period of 30 min led to the maximum radiolabelling yield of 98.0%, without any noticeable change while raising the response time above the optimum (30 min) [27]. Moreover, the radiolabelling yield greatly increased up to a maximum of 50 µg of tin (II) content (optimum content), reaching a value of 98.0%. Tin (II) content greater than 50 µg may lead to the formation of an undesirable colloid. Ultimately, the *in vitro* stability of [^{99m}Tc]dithiocarbamate of famotidine complex was investigated in rat serum. The radiotracer, [^{99m}Tc]dithiocarbamate of famotidine complex, was shown to be stable for 24 h with no discernible alteration. After 12 h, the stability decreased to 95%, and then dropped to 94% after 24 h, Table 1 [41–45].

3.3 Blocking study of histamine-2-receptor antagonists (H_2RAs)

Famotidine (250–1000 µg) was utilized to pre-dose animals with unlabelled famotidine 30 min before the injection of

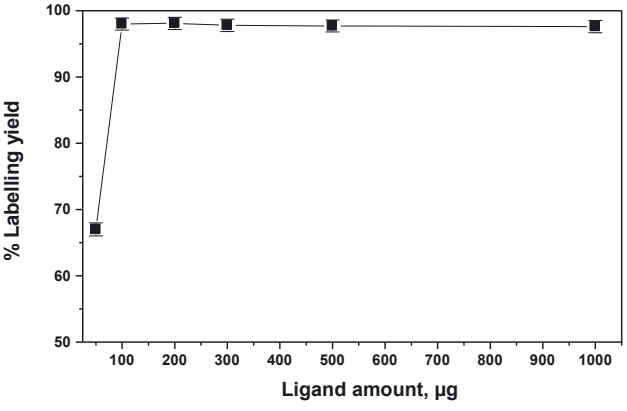

Figure 5: Effect of amount of dithiocarbamate of famotidine (in %) on the radiolabelling yield % of [^{99m}Tc]dithiocarbamate of famotidine complex. Conditions: 50–1000 µg of famotidine, 50 µg Sn (II), pH 5 and 30 min reaction time, (mean yield % ± SD, n = 3). The curve is an eye-guide.

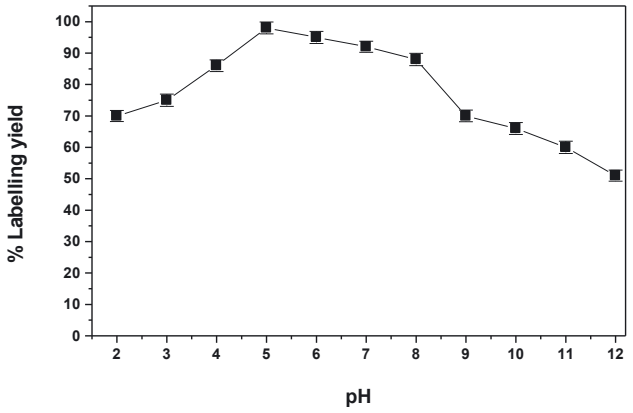

Figure 6: Effect of pH on the radiolabeling yield of [99mTc] dithiocarbamate of famotidine complex. Conditions: 100 µg of famotidine, 50 µg Sn (II), pH (2–12) and 30 min reaction time, (mean yield % ± SD, $n = 3$). The curve is an eye-guide.

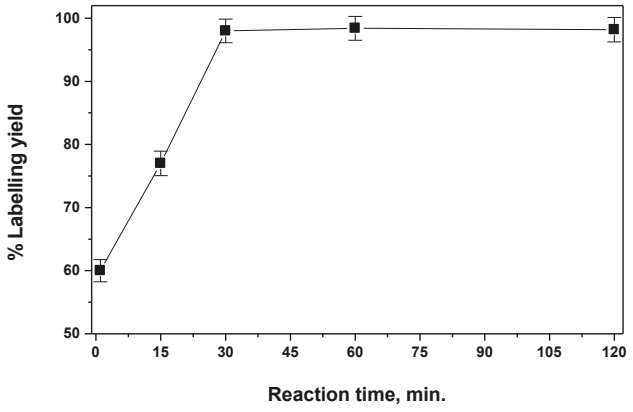

Figure 7: Effect of reaction time on the radiolabelling yield % of [99mTc]dithiocarbamate of famotidine complex. Conditions: 100 µg of famotidine, 50 µg Sn (II), pH 5 and (1–120) min reaction time, (mean yield % ± SD, $n = 3$). The curve is an eye-guide.

hot [99mTc]dithiocarbamate of famotidine complex, which reduced ulcerated stomach uptake from 68 to 8% ID/g organ at 30 min after injection. The thermally tagged molecule, [99mTc]dithiocarbamate of famotidine complex, binds specifically with H_2RAs in the stomach. As a consequence of this research, [99mTc]dithiocarbamate of famotidine complex can be successfully used in imaging of histamine-2-receptor antagonists in mice (Figure 8) [46–50].

3.4 Biodistribution study

Table 2 shows the biodistribution of [99mTc]dithiocarbamate of famotidine complex in different body organs and fluids of normal mice. All radioactivity levels are expressed as an average percent-injected dose per organ tissue (%ID/g

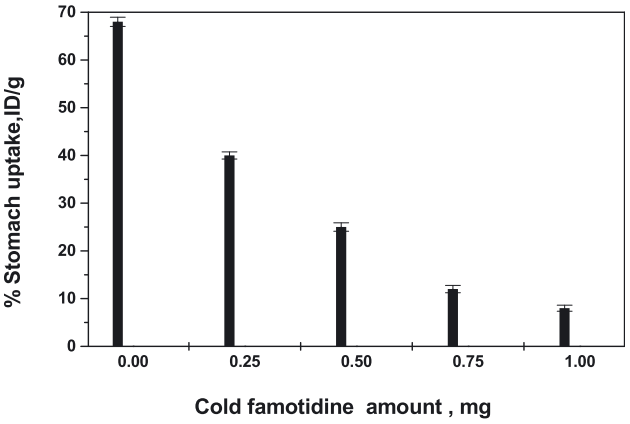

Figure 8: Inhibition of uptake of [99mTc]dithiocarbamate of famotidine complex by stomach as a function of amount of preinjected famotidine in normal male Swiss Albino mice at 30 min post injection (%ID/g ± SD, $n = 5$).

organ ± SD), in comparison to the activity in a standard solution of the labelled substrate at the time of examination [51–55]. The kidneys' uptake was found to be 35% at 60 min and reduced to 3.17% at 24 h post injection (p.i.). Therefore, the labelled compound, [99mTc]dithiocarbamate of famotidine complex, is excreted mainly through the urinary pathway system [56–58]. The radiotracer, [99mTc]dithiocarbamate of famotidine complex, is distributed rapidly in most organs at 30 min post injection [59–66]. The stomach uptake was found to be 8.28% at 30 min post injection and decreased to 2.25% at 24 h post injection. Therefore, this could be considered as a new period for stomach imaging at a new appropriate time that is superior to several radiotracers [4–12].

Table 3 shows the biodistribution of [99mTc]dithiocarbamate of famotidine complex in ulcer-bearing mice. This biological distribution clearly shows that there is no variation between Tables 2 and 3 except for the concentration of the labelled component, [99mTc]dithiocarbamate of famotidine complex in the ulcerated stomach. As a result, it is critical to compare the uptake of the labelled chemical, [99mTc]dithiocarbamate of famotidine complex concentration, in ulcerated and non-ulcerated stomachs in both modes. Table 3 shows that the ulcer stomach uptake was 68% at 30 min post injection and remained high to 27.15% at 24 h post injection, which was higher than the normal stomach uptake (Table 2).

We compare this ulcer stomach uptake of [99mTc] dithiocarbamate of famotidine complex (68% at 30 min p.i.), % ID/g organ ± SD, value with some published labelled compounds such as [131I]rabeprazole (33.5% at 30 min p.i.) [6], [125I]famotidine (65.9% at 30 min p.i.) [5], [125I]omeprazole (28.0% at 30 min p.i.) [13], [125I]cimetidine (30.12% at 30 min p.i.) [11], [99mTc]rabeprazole (33.4% at 30 min p.i.) [9], [99mTc]pantoprazole (27.2% at 30 min p.i.)

Table 2: Biodistribution of [^{99m}Tc]dithiocarbamate of famotidine complex in normal mice.

Organ or body fluid	Percent ID/g organ					
	Time post injection					
	30 min	60 min	2 h	4 h	8 h	24 h
Blood	5.11 ± 0.09	3.15 ± 0.06	2.15 ± 0.13	1.44 ± 0.03	1.00 ± 0.12	0.95 ± 0.00
Bone	1.11 ± 0.15	1.10 ± 0.03	0.99 ± 0.00	0.95 ± 0.00	0.90 ± 0.00	0.83 ± 0.00
Muscle	1.15 ± 0.02	1.17 ± 0.08	1.11 ± 0.01	0.99 ± 0.00	0.95 ± 0.00	0.85 ± 0.00
Liver	3.15 ± 0.25	4.99 ± 0.05	4.22 ± 0.46	3.43 ± 0.22	3.10 ± 0.37	2.10 ± 0.07
Lung	1.0 ± 0.02	1.11 ± 0.03	0.99 ± 0.00	0.98 ± 0.00	0.80 ± 0.00	0.77 ± 0.00
Heart	1.15 ± 0.02	1.13 ± 0.01	1.11 ± 0.08	0.98 ± 0.0	0.97 ± 0.0	0.90 ± 0.0
Stomach	8.28 ± 0.11	6.30 ± 0.24	5.22 ± 0.18	4.15 ± 0.21	3.17 ± 0.31	2.25 ± 0.12
Intestine	3.12 ± 0.03	5.90 ± 0.01	4.11 ± 0.12	3.20 ± 0.09	2.15 ± 0.02	1.90 ± 0.07
Kidney	18.19 ± 0.36	35 ± 0.66	24.18 ± 0.27	12.40 ± 0.98	6.12 ± 0.27	3.17 ± 0.49
Spleen	1.12 ± 0.05	1.10 ± 0.01	0.99 ± 0.00	0.97 ± 0.00	0.95 ± 0.01	0.90 ± 0.00

Values represent mean ± SEM, $n = 3$.

Table 3: Intravenous biodistribution of [^{99m}Tc]dithiocarbamate of famotidine complex in ulcer bearing mice.

Organ or body fluid	Percent ID/g organ					
	Time post injection					
	30 min	60 min	2 h	4 h	8 h	24 h
Blood	5.16 ± 0.02	3.17 ± 0.02	2.18 ± 0.11	1.97 ± 0.01	1.12 ± 0.12	0.98 ± 0.00
Bone	1.12 ± 0.11	1.13 ± 0.01	1.11 ± 0.02	0.97 ± 0.00	0.91 ± 0.00	0.87 ± 0.00
Muscle	1.13 ± 0.01	1.11 ± 0.02	1.00 ± 0.03	0.94 ± 0.00	0.90 ± 0.00	0.89 ± 0.00
Liver	3.19 ± 0.04	5.11 ± 0.06	4.96 ± 0.33	3.11 ± 0.08	2.92 ± 0.06	2.15 ± 0.03
Lung	1.3 ± 0.01	1.23 ± 0.04	1.11 ± 0.01	1.00 ± 0.02	0.89 ± 0.00	0.80 ± 0.00
Heart	1.12 ± 0.01	1.10 ± 0.07	1.00 ± 0.01	0.90 ± 0.01	0.88 ± 0.0	0.80 ± 0.0
Stomach	68 ± 0.67	45.11 ± 0.68	39.25 ± 0.13	35.19 ± 0.27	29.15 ± 0.96	27.15 ± 0.19
Intestine	3.19 ± 0.01	5.44 ± 0.05	4.77 ± 0.09	3.25 ± 0.04	2.19 ± 0.01	1.80 ± 0.04
Kidney	19.15 ± 0.57	34.80 ± 0.90	27.15 ± 0.66	14.50 ± 0.78	7.11 ± 0.33	3.15 ± 0.05
Spleen	1.10 ± 0.07	1.00 ± 0.04	0.99 ± 0.00	0.96 ± 0.00	0.91 ± 0.01	0.87 ± 0.00

Values represent mean ± SEM, $n = 3$.

[7], [^{99m}Tc]esomeprazole (16.33% at 30 min p.i.) [10], [^{99m}Tc] omeprazole (22% at 60 min p.i.) [8] and ^{99m}Tc-tannic acid (15% at 120 min p.i.,max. value). According to the findings of this investigation, the labelled compound, [^{99m}Tc] dithiocarbamate of famotidine complex, has a higher % ID/g organ ± SD value than other materials [4–14].

4 Conclusions

The labelling conditions of the molecule, [^{99m}Tc]dithiocarbamate of famotidine complex, have been improved for the production with high radiolabelling yield of 98% and high stability in rat serum. According to biodistribution experiments in mice, the radiotracer under investigation has a high ulcer stomach absorption of 68% ID/g at 30 min post-injection. This ID/organ value is greater than those of other newly discussed agents according to Refs. [4–14]. Therefore, the radiotracer [^{99m}Tc]dithiocarbamate of famotidine complex might be considered a new possible selective radiotracer for ulcerated stomach imaging.

Author contributions: All the authors have accepted responsibility for the entire content of this submitted manuscript and approved submission.

Research funding: None declared.

Conflict of interest statement: The authors declare no conflicts of interest regarding this article.

References

1. Howard J. M., Chremos A. N., Collen M. J., McArthur K. E., Cherner J. A., Maton P. N., Ciarleglio C. A., Cornelius M. J., Gardner J. D., Jensen R. T. Famotidine, a new, potent, longacting histamine H_2-receptor antagonist: comparison with cimetidine

and ranitidine in the treatment of Zollinger-Ellison syndrome. *Gastroenterology* 1985, *88*, 1026–1033.
2. Meskanen K., Ekelund H., Laitinen J., Neuvonen P. J., Haukka J., Panula P., Ekelund J. A. Randomized clinical trial of histamine 2 receptor antagonism in treatment-resistant schizophrenia. *J. Clin. Psychopharmacol.* 2013, *33*, 472–478.
3. James L. P., Marshall J. D., Heulitt M. J., Wells T. G., Letzig L., Kearns G. L. Pharmacokinetics and pharmacodynamics of famotidine in children. *J. Clin. Pharmacol.* 1996, *36*, 48–54.
4. Sanad M. H., Saleh G. M., Marzook F. A. Radioiodination and biological evaluation of nizatidine as a new highly selective radiotracer for peptic ulcer disorder detection. *J. Label. Compd. Radiopharm.* 2017, *60*, 600–607.
5. Sanad M. H., Salama D. H., Marzook F. A. Radioiodinated famotidine as a new highly selective radiotracer for peptic ulcer disorder detection, diagnostic nuclear imaging and biodistribution. *Radiochim. Acta* 2017, *105*, 389–398.
6. Sanad M. H., Challan S. B. Radioiodination and biological evaluation of rabeprazole as a peptic ulcer localization radiotracer. *Radiochemistry* 2017, *59*, 307–312.
7. Sanad M. H., Ibrahim I. T. Radiodiagnosis of peptic ulcer with technetium-^{99m} pantoprazole. *Radiochemistry* 2013, *55*, 341–345.
8. Sanad M. H. Labeling of omeprazole with technetium-^{99m} for diagnosis of stomach. *Radiochemistry* 2013, *55*, 605–609.
9. Sanad M. H., Ibrahim I. T. Radiodiagnosis of peptic ulcer with technetium-^{99m} labeled rabeprazole. *Radiochemistry* 2015, *57*, 425–430.
10. Sanad M. H., Talaat H. M. Radiodiagnosis of peptic ulcer with technetium-^{99m}-labeled esomeprazole. *Radiochemistry* 2017, *59*, 396–401.
11. Sanad M. H., Safaa B. C., Fawzy A. M., Sayed M. A. A., Ebtisam A. M. Radioiodination and biological evaluation of cimetidine as a new highly selective radiotracer for peptic ulcer disorder detection. *Radiochim. Acta* 2021, *109*, 109–117.
12. Unak P., Lambrecht F. Y., Biber F. Z., Medine I. E., Teksoz S. Labeling of famotidine with ^{99m}Tc and biodistribution studies on rats. *J. Radioanal. Nucl. Chem.* 2004, *261*, 587–591.
13. Amin A. M., Omar M. M., Abd-Elhaliem S. M., Elshanawany A. A. Gastric ulcer localization: potential use of ^{125}I-omeprazole as radiotracer. *Radiochemistry* 2015, *57*, 182–186.
14. Ibrahim I. T., El-Tawoosy M., Talaat H. M. Labeling of tannic acid with technetium-^{99m} for diagnosis of stomach ulcer. *Int. Sch. Res. Netw.* 2011, *2011*, 1–6.
15. Sanad M. H., Sallam K. M., Marzook F. Labeling and biological evaluation of ^{99m}Tc-tricarbonyl-chenodiol for hepatobiliary imaging. *Radiochemistry* 2017, *59*, 525–529.
16. Song X., Wang Y., Zhang J. Influence of different ^{99m}Tc cores on the physicochemical and biodistribution behaviours of ^{99m}Tc-labelled complexes of pamidronate dithiocarbamate. *J. Radioanal. Nucl. Chem.* 2018, *316*, 313–319.
17. Krishnaveni G., Sathyannarayana P. V. V. Simultaneous determination of famotidine and ibuprofen in combined pharmaceutical dosage form by RP-HPLC method. *Int. J. Pharm. Bio. Sci.* 2013, *4*, 655–662.
18. Sanad M. H., Farouk N., Fouzy A. S. M. Radiocomplexation and bioevaluation of ^{99m}Tc nitrido-piracetam as a model for brain imaging. *Radiochim. Acta* 2017, *105*, 729–737.
19. Sanad M. H., Alhussein A. I. Preparation and biological evaluation of ^{99m}TcN-histamine as a model for brain imaging: in silico study and preclinical evaluation. *Radiochim. Acta* 2018, *106*, 229–238.
20. Sanad M. H. Novel radiochemical and biological characterization of ^{99m}Tc-histamine as a model for brain imaging. *J. Anal. Sci. Technol.* 2014, *5*, 23.
21. Xiang L., Aiqin W., Qianqian X., Yu F., Jianping L., Huabei Z., Huaying B. Synthesis and biological evaluation of fatty acids containing ^{99m}Tc-oxo and ^{99m}Tc-nitrido for myocardial metabolism imaging. *J. Radioanal. Nucl. Chem.* 2016, *307*, 1438.
22. Duatti A., Boschi A., Uccelli L. Technetium -^{99m} nitrido radiopharmaceuticals with un precedented biological properties. *Braz. Arch. Biol. Technol.* 2002, *45*, 135–142.
23. Boschi A., Uccelli L., Bolzati C., Duatti A., Sabba N., Moretti E., Domenico G. D., Zavattini G., Refosco F., Giganti M. Synthesis and biologic evaluation of monocationic asymmetric ^{99m}Tc-nitride heterocomplexes showing high heart uptake and improved imaging properties. *J. Nucl. Med.* 2003, *44*, 806–814.
24. Zhang J. B., Wang X. B., Tian C. J. Synthesis and biodistribution of ^{99m}TcN $(PDTC)_2$ as a potential brain imaging agent. *J. Radioanal. Nucl. Chem.* 2004, *262*, 505–507.
25. Zhang J. B., Luo G., Wang X. B. Synthesis and biodistribution of a novel ^{99m}Tc nitrido dithiocarbamate complex containing ether group as a potential myocardial and brain imaging agent. *J. Radioanal. Nucl. Chem.* 2009, *279*, 783–785.
26. Mingxia Z., Hongyu N., Man F., Shilei L., Jin C., Chuanmin Q. Novel $[^{99m}TcN]^{2+}$ labeled EGFR inhibitors as potential radiotracers for single photon emission computed tomography (SPECT) tumor imaging. *Molecules* 2014, *19*, 5508–5521.
27. Zhang J. B., Wang X. B., Tian C. J. Synthesis of a bis-(*N*-butyldithiocarbamato)- nitrido ^{99m}Tc complex: a potential new brain imaging agent. *J. Radioanal. Nucl. Chem.* 2007, *273*, 15–17.
28. Guleria M., Ghosh S., Das T., Sarma H. D., Banerjee S. Preparation and bioevaluation of $[^{99m}Tc{\equiv}N]^{2+}$ labeled tetrameric complex of E c(RGDfK)$_2$ as a radiotracer for imaging avb3 integrins in tumors. *J. Radioanal. Nucl. Chem.* 2016, *309*, 923–930.
29. Shah S. Q., Khan M. R., Ali S. M. Radiosynthesis of ^{99m}Tc $(CO)_3$-clinafloxacin dithiocarbamate and its biological evaluation as a potential staphylococcus aureus infection radiotracer. *Nucl. Med. Mol. Imag.* 2011, *45*, 248–254.
30. Xiang L., Aiqin W., Qianqian X., Yu F., Jianping L., Huabei Z., Huaying B. Synthesis and biological evaluation of fatty acids containing ^{99m}Tc-oxo and ^{99m}Tc-nitrido for myocardial metabolism imaging. *J. Radioanal. Nucl. Chem.* 2016, *307*, 1429–1438.
31. Mathur A., Mallia M. B., Subramanian S., Banerjee S., Kothari K., Dhotare B., Sarmad H. D., Venkatesh M. ^{99m}TcN complexes of tert-butyl dithiocarbamate and methoxyisobutyl dithiocarbamate as myocardial and brain imaging agents. *Nucl. Med. Commun.* 2005, *26*, 1013–1019.
32. Pasqualini R., Comazzi V., Bellande E., Duatti A., Marrchi A. A new efficient method for the preparation of ^{99m}Tc-radiopharmaceuticals containing the Tc≡N multiple bond. *Appl. Radiat. Isot.* 1992, *43*, 1329–1333.
33. Sanad M. H., Rizvi S. F. A., Farag A. B. Synthesis, characterization, and bioevaluation of ^{99m}Tc nitrido-oxiracetam as a brain imaging model. *Radiochim. Acta* 2021, *109*, 477–483.
34. Borai E. H., Sanad M. H., Fouzy A. S. M. Optimized chromatographic separation and biological evaluation of ^{99m}Tc-clarithromycin for infective inflammation diagnosis. *Radiochemistry* 2016, *58*, 84–91.
35. Wang R., Zeng X., Liu B., Yi R., Zhou X., Mu J., Zhao X. Prophylactic effect of Lactobacillus plantarum KSFY06 on HCl/ethanol-induced gastric injury in mice. *Food Funct.* 2020, *11*, 2679–2692.

36. Sanad M. H. Labeling and biological evaluation of ^{99m}Tc-azithromycin for infective inflammation diagnosis. *Radiochemistry* 2013, *55*, 539–544.
37. Sanad M. H., Sallam Kh. M., Marzook F. A., Abd-Elhaliem S. M. Radioiodination and biological evaluation of candesartan as a tracer for cardiovascular disorder detection. *J. Label Compd. Radiopharm.* 2016, *59*, 484–491.
38. Abdel-Ghaney I. Y., Sanad M. H. Synthesis of ^{99m}Tc-erythromycin complex as a model for infection sites imaging. *Radiochemistry* 2013, *55*, 418–422.
39. Ibrahim I. T., Sanad M. H. Radiolabeling and biological evaluation of losartan as a possible cardiac imaging agent. *Radiochemistry* 2013, *55*, 336–340.
40. Motaleb M. A., Adli A. S. A., El-Tawoosy M., Sanad M. H., AbdAllah M. An easy and effective method for synthesis and radiolabelling of risedronate as a model for bone imaging. *J. Label Compd. Radiopharm.* 2016, *59*, 157–163.
41. Sanad M. H., El-Bayoumy A. S. A., Alhussein A. I. Comparative biological evaluation between $^{99m}Tc(CO)_3$ and ^{99m}Tc-Sn(II) complexes of novel quinoline derivative: a promising infection radiotracer. *J. Radioanal. Nucl. Chem.* 2017, *311*, 1–14.
42. Sanad M. H., Emad H. B. Comparative biological evaluation between ^{99m}Tc tricarbonyl and ^{99m}Tc-Sn(II) levosalbutamol as a β2-adrenoceptor agonist. Radiochim. Acta 2015, *103*, 879–891.
43. Sanad M. H., El-Tawoosy M. Labeling of ursodeoxycholic acid with Technetium-99m for hepatobiliary imaging. *J. Radioanal. Nucl. Chem.* 2013, *298*, 1105–1109.
44. Amin A. M., Sanad M. H., Abd-Elhaliem S. M. Radiochemical and biological characterization of ^{99m}Tc-piracetam for brain imaging. *Radiochemistry* 2013, *55*, 624–628.
45. El-Kawy O., Sanad M. H., Marzook F. ^{99m}Tc-Mesalamine as potential agent for diagnosis and monitoring of ulcerative colitis: labelling, characterisation and biological evaluation. *J. Radioanal. Nucl. Chem.* 2016, *308*, 279–286.
46. Sanad M. H., Amin A. M. Optimization of labeling conditions and bioevalution of ^{99m}Tc-meloxicam for inflammation imaging. *Radiochemistry* 2013, *55*, 521–526.
47. Sanad M. H., Sakr T. M., Walaa H. A. A., Marzook E. A. In silico study and biological evaluation of ^{99m}Tc-tricabonyl oxiracetam as a selective imaging probe for AMPA receptors *J. Radioanal. Nucl. Chem.*, 2017, *314*, 1505–1515.
48. Sanad M. H., Farag A. B., Dina H. S. J. Radioiodination and bioevaluation of rolipram as a tracer for brain imaging: in silico study, molecular modeling and gamma scintigraphy. *J. Label Compd. Radiopharm.* 2018, *61*, 501–508.
49. Sanad M. H., Abelrahman M. A., Marzook F. M. A. Radioiodination and biological evaluation of levalbuterol as a new selective radiotracer: a β2-adrenoceptor agonist. *Radiochim. Acta* 2016, *104*, 345–353.
50. Sanad M. H., Marzook E. A., Challan S. B. Radioiodination of olmesartan medoxomil and biological evaluation of the product as a tracer for cardiac imaging. *Radiochim. Acta* 2018,*106*, 329–336.
51. Motaleb, M. A., Selim, A. A., El-Tawoosy, M., Sanad M. H., El-Hashash, M. A. Synthesis, radiolabeling and biological distribution of a new dioxime derivative as a potential tumor imaging agent. *J. Radioanal. Nucl. Chem.*. 2017, *314,* 1517–1522.
52. Moustapha, M. E., Motaleb, M. A. & Sanad, M. H. Synthesis and biological evaluation of ^{99m}Tc-labetalol for β1-adrenoceptor-mediated cardiac imaging. *J. Radioanal. Nucl. Chem.* 2016, *309*, 511–516.
53. Sanad M. H., Ibrahim A. A., Talaat H. M. Synthesis, bioevaluation and gamma scintigraphy of ^{99m}Tc-N-2-(Furylmethyl iminodiacetic acid) complex as a new renal radiopharmaceutical. *J. Radioanal.Nucl. Chem.* 2018, *315*, 57–63.
54. Sanad M. H., Emad H. B. Performance characteristics of biodistribution of ^{99m}Tc-cefprozil for in-vivo infection imaging. *J. Anal. Sci. Technol.* 2014, *5*, 32.
55. Sanad H. M., Ibrahim A. A. Radioiodination, diagnostic nuclear imaging and bioevaluation of olmesartan as a tracer for cardiac imaging. *Radiochim. Acta* 2018, *106*, 843–850.
56. Safaa B. C., Fawzy A. M., Ayman M. Synthesis of radioiodinated carnosine for hepatotoxicity imaging induced by carbon tetrachloride and its biological assessment in rats. *Radiochim. Acta* 2021, *108*, 397–408.
57. Sanad M. H., Sallam K. M., Marzook F. Labeling and biological evaluation of ^{99m}Tc-tricarbonyl-chenodiol for hepatobiliary imaging. *Radiochemistry* 2017, *59*, 525–529.
58. Sanad M. H., Fouzy A. S. M., Sobhy H. M., Hathout A. S., Hussain O. A. Tracing the protective activity of Lactobacillus plantarum using technetium-99m-labeled zearalenone for organ toxicity. *Int. J. Radiat. Biol.* 2018, *94*, 1151–1158.
59. Sanad M. H., Farag A. B., Saleh G. M. Radiosynthesis and biological evaluation of ^{188}Re-5,10,15,20–Tetra (4-pyridyl)-21H,23H-porphyrin complex as a tumor-targeting agent. *Radiochemistry* 2019, *61*, 347–351.
60. Sanad M. H., Marzook F. A., Abd-Elhaliem S. M. Radioiodination and biological evaluation of irbesartan as a tracer for cardiac imaging. *Radiochim. Acta* 2021, *109*, 41–46.
61. Elham M. H., Eyssa H. M., Abd El-Megeed A. A. Effect of nanofiller on the ageing of rubber seal materials under gamma irradiation. *J. Compos. Mater.* 2019, *53*, 2065.
62. Eyssa H. M., Dalia E. A., Mervat A. M. Abo-State. Application of polyurethane/gamma-irradiated carbon nanotubes composites as antifouling coat. Polym. Compos. 2018, *39*, E1196.
63. Sanad M. H., Rizvi F. A., Kumar R. R. Radiosynthesis and bioevaluation of ranitidine as highly selective radiotracer for peptic ulcer disorder detection. *Radiochemistry* 2020, *62*, 119–124.
64. Eyssa H. M., Mohamed W. S., Mai M El-Zayat M. M. Irradiated rubber composite with nano and micro fillers for mining rock application. *Radiochimica Acta* 2019, *107*, 737–753.
65. Zaky M. M., Eyssa H. M., Sadek R. F. Improvement of the magnesium battery electrolyte properties through gamma irradiation of nano polymer electrolytes doped with magnesium oxide nanoparticles. *Journal of Vinyl and Additive Technology* 2019, *25*, 243–254.
66. Eyssa H. M., Sawires S. G., Senna M. M. Gamma irradiation of polyethylene nanocomposites for food packaging applications against stored-product insect pests. *Journal of Vinyl and Additive Technology* 2019, *25*, E120–E129.